STOYAN NEDELTCHEV, JAKUB KATERLA

DETERMINATION OF ALL HYDRODYNAMICALLY STABLE AND EASILY PREDICTABLE CONDITIONS IN VARIOUS BUBBLE COLUMNS

Institute of Chemical Engineering, Polish Academy of Sciences, Bałtycka 5, 44-100 Gliwice, Poland

The reliable operation of bubble columns depends on the selection of hydrodynamically stable conditions. They have been defined based on the fully predictable behavior of an identification parameter in a certain gas velocity range. In order to define these stable conditions, three key parameters (Kolmogorov entropy, new hybrid index and information entropy) have been extracted from various intrusive and non-intrusive measurements in water, ethanol, therminol LT and benzonitrile.

Keywords: hydrodynamically stable bubble columns, different entropies, new hybrid index

Optymalny zakres pracy kolumn barbotażowych zależy od wyboru warunków hydrodynamicznej stabilności. Warunki te zostały zdefiniowane w oparciu o całkowitą przewidywalność zachowania się parametru charakterystycznego w określonym zakresie prędkości gazu. W celu identyfikacji warunków stabilności wyodrębniono z różnych inwazyjnych i nieinwazyjnych pomiarów w wodzie, etanolu, terminolu LT i benzonitrylu trzy kluczowe parametry – entropię Kołmogorowa, nowy indeks hybrydowy i entropię informacji.

Słowa kluczowe: kolumny barbotażowe stabilne hydrodynamicznie, entropia, nowy indeks hybrydowy

1. INTRODUCTION

Bubble columns (BCs) are widely used in chemical, petrochemical and biochemical industries as well as wastewater treatment. These gas-liquid contactors find broad applications in industry due to their salient advantages i.e. no moving parts (simple design), low operational cost and ease of maintenance. Moreover, BCs are characterized by high mass and heat transfer coefficients. In the chemical industry, these gas-liquid contactors might be used not only for different reactions such as oxidation, hydrogenation, chlorination or alkylation but also absorption and wastewater treatment. In these columns the gas is being distributed through the liquid phase or, in so-called slurry BCs,

through the liquid-solid suspension [1], [2]. These reactors are characterized by complicated hydrodynamics and many factors have impact on the bubble bed behavior, including working conditions (temperature and pressure), properties of gas and liquid, column and gas distributor shape and dimensions [3]. BCs might operate in co- or countercurrent flow of gas and liquid. This is why the gas (and liquid – in case of liquid flow) velocity also affects the BC hydrodynamics.

The BC design depends on three aspects: mass and heat transfer, mixing characteristics and chemical kinetics of reaction [2]. It is noteworthy that not every process in bubble columns is a chemical reaction; physical processes also occur (e.g. absorption of gas in liquid). Another parameters which take responsibility for complexity of fluid dynamics in the columns are gas-liquid interfacial area, dispersion coefficients, gas holdup or bubble diameter. This is the reason why the design and scale-up of BCs is a challenging task and matter of interest for many authors.

BCs operate in different hydrodynamic flow regimes which depends mostly on superficial gas velocity U_g. Another significant factor is the gas distributor type, especially in the homogeneous regime [4]. In ambient conditions three main flow regimes can be distinguished: (i) homogeneous (bubbly), (ii) transition and (iii) heterogeneous (churn-turbulent) [5]. All of them are characterized with different flow patterns. The flow regime has an influence on the interfacial area between the phases and mass and heat transfer, thus on the effectiveness of BC performance. Therefore, the transition between the flow regimes is a matter of great importance and crucial design parameter [6]. During homogenous regime the phenomena of bubble coalescence or break-up do not occur and bubbles are small, uniformly sized (with an ellipsoidal shape) and regularly distributed over the cross-sectional area [7]. Also the bubble size distribution (BSD) is narrow, the profile of gas holdup is flat and low turbulence in the bubble bed is observed [3]. Opposite to the homogeneous regime, the heterogeneous regime is characterized by wide BSD, parabolic gas holdup profile and occurrence of bubble coalescence and brake-up. Also liquid circulation might be observed during the heterogeneous regime, while the liquid is rising in the core of the column and moving down in the vicinity of walls [8]. In the churn-turbulent flow regime ellipsoidal (in the annulus) or spherical-cap (in the core) shapes are also observed and bubble rise velocity is higher. Furthermore in the homogeneous regime only “small” bubbles exist, while in the heterogeneous two bubble classes: “small” and “large”, co-exist in the bubbly bed [9]. These differences are the basis for distinction of flow regimes via visual observation. Bubbles shape and size are essential for the stability of the hydrodynamic regime [10]. Occurrence of both small and large bubbles leads to a division in gas holdup, i.e. “dense” and “dilute” phase gas holdups for small and large bubbles are defined, respectively [11]. In the dense phase the small bubbles are uniformly distributed in the cross-section and along the axis of the column and the bubble rise velocity is low. Transition regime occurs between homogeneous and heterogeneous regimes, but it is not simple to describe its characteristics as far as the flow regime transition is a gradual process. Therefore there is a need to study and clarify the stability conditions of both flow regimes [12]. Apart

from visual observations, another method for simple assessment of transition points is plotting a figure of gas holdup versus U_g, what has been reported by many authors [1], [13], but it is not always a reliable practice. Usually the gas holdup in water in homogeneous regime increases approximately linearly and changes this linear correlation to form plateau with transition to heterogeneous regime. The occurrence of the first large bubble is responsible for that fact, because these bubbles have higher rise velocity, therefore they exit faster from the bubble bed.

It is difficult to predict the BC behavior due to their complicated hydrodynamics. For instance, in these gas-liquid contactors the bubble shape and the bubble size distribution can vary with both time and location [14].

The unstable oscillations of the flow rate usually generate irregular flow patterns. When pressure fluctuations are measured, signal instabilities are observed, which correspond to the irregular flow patterns. It is common to observe more intensive fluctuations in some parts of the signal when both the gas flow rate and the flow patterns are unstable. In principle, the availability of more orifices in the gas distributor favors the homogeneity of the flow, reducing the flow pattern instabilities.

When a characteristic parameter exhibits practically the same values at different gas flow rates, it means that the flow patterns have the same structure and they are exposed to minor instabilities. In other words, the unstable flow behavior and the signal oscillations are interrelated. The instability in the flow patterns is also related to the turbulence intensity in the reactor.

It is worth noting that the recirculation loops (typical for the heterogeneous flow regime) and unstable vortices cause more oscillations in the signals (pressure fluctuations) and thus more instabilities in the signal's profile as a function of U_g. In principle, the increase of the Reynolds number favors more intensive pressure oscillations. They are associated with higher turbulent dissipation, which is attributable to higher number of small uncontrollable eddies.

Many of the irregularities in the signal are caused by the uncontrolled instabilities of the gas flow rate. So, recordings for a very long time are not very useful due to the impossibility of achieving a constant flow rate over long periods.

It is very important to understand better the behaviors of the gas-liquid dispersion and the impact that they have on the flow instabilities. It should be precisely determined the operating conditions at which the transition between the different flow regimes occur.

The tall BCs should be very well investigated since under these conditions always some irregularities of the flow pattern are observed. They contribute to the flow regime instabilities. Most of the industrial BCs have high bed aspect ratios.

The hydrodynamic stability in the BC is related to the circulation pattern in the bubble bed [14]. The authors have introduced a stability criterion and based on it was found that the instability at the bottom zone was induced by the low-frequency meandering of the bubble swarm. The unstable behavior of BCs is associated with the turbulence characteristics of the liquid phase at different U_g values.

The instabilities and irregularities in the signal are more pronounced in the heterogeneous regime. Under these turbulent conditions, most of the ascending bubbles are centralized in a small area. Large-scale and strong non-uniformities in the buoyancy distribution drive large-scale and strong convective motions of liquid and bubbles inside the BC [14]. The increased U_g values promote more intensive bubble-bubble hydrodynamic interactions.

The main objective of this work is to identify all hydrodynamically stable and easily predictable operating conditions in various BCs. For this purpose, the behavior of several reliable identification parameters (Kolmogorov entropy (KE), new hybrid index (NHI) and information entropy (IE)) has been investigated. These parameters have been extracted from the fluctuations (time series) of different signals (pressure, temperature, gas holdup and photon counts). Measurements in tap water, deionized water, ethanol (96 %), benzonitrile and therminol LT have been performed.

2. PARAMETERS DESCRIPTION

2.1. KOLMOGOROV ENTROPY

The Kolmogorov entropy (KE) quantifies the degree of unpredictability of the system. In the case of BCs, the system is the gas-liquid dispersion. The KE is associated with the rate of information loss of the system. KE > 0 is a sufficient condition for chaos. The time behavior of the gas-liquid dispersion in the BC is described as chaotic when that behavior is aperiodic and apparently random. The chaotic system (such as a BC) is only predictable over a restricted time interval. This chaotic parameter is sensitive to even small changes in the operating conditions. A high value of KE implies a very irregular dynamic behavior, while small KE value corresponds to more regular, periodic-like behavior. In the case of completely periodic systems, KE is equal to zero. The most important concept to analyze chaos from a complex time series (for instance, pressure fluctuations) is to unfold the hidden chaotic attractor. The KE value characterizes this figure. The attractor of a chaotic system is not finite and the system never returns to the same state. Van den Bleek and Schouten [15] have developed a reliable technique for attractor reconstruction. In addition, Schouten et al. [16] have published their well-known approach for KE estimation. The signal has been divided into different vectors (consisting of certain number of elements) and then many different vector pairs have been generated. The distances between these vector pairs have been estimated based on the maximum norm definition. Only the vector pairs with a distance smaller than a preselected characteristic value (set equal to the average absolute deviation (AAD)) have been taken into account in the KE estimation. The number of steps it takes for two state vectors to deviate exponentially from each other determines the local b value. The number of these values b_{avg} takes part in the KE estimation:

$$KE = sampling\ frequency\left(1 - \frac{1}{b_{avg}}\right) \tag{1}$$

Schouten et al. [16] have recommended that at least 10 000 vector pairs are considered in order to have a reliable KE value.

2.2. NEW HYBRID INDEX

This dimensionless parameter has been applied to gas holdup fluctuations. The gas holdup time series (4000 points) has been divided into 8 different periods consisting of 500 points. Then, the average absolute deviation (AAD) in each period has been estimated. AAD is a robust statistical estimator of the data width around the mean. It is a sum of all absolute differences $|x_j\text{-}x_{mean}|$ divided by the total number of points in the time series.

Further, the probability P_i for having such a data sequence yielding a particular AAD in each period has been calculated as a ratio of the AAD in that period divided by the sum of all AAD values:

$$P_i = AAD_i \,/\, \sum_{i=1}^{N} AAD_i \tag{2}$$

The information amount IA_i in each period has been calculated by means of Eq. (3):

$$IA_\mathrm{i} = -\log(P_i) \tag{3}$$

The new hybrid index represents the following ratio:

$$NHI = \left|\sum_{i=1}^{N} IA_\mathrm{i} - \sum_{i=1}^{N} AAD_i\right| / \sum_{i=1}^{N} AAD_i \tag{4}$$

At low U_g values the NHI is much higher than 1. However, at U_g values beyond 0.025 m/s it varies between 0 and 1. The NHI value characterizes the statistical non-uniformity in the measured signal. At the main regime transition velocity the signals are better ordered, i.e. statistically more uniform [17].

2.3. INFORMATION ENTROPY

The newly defined information entropy (IE) algorithm will be applied to temperature fluctuations recorded in an annularly aerated BC. The main originality is that it will be applied to AAD values extracted from 6 intervals consisting of 100 points from the recorded temperature fluctuations (600 points). Then the probability P_i for the occurrence of certain local temperature values and local AAD will be calculated by means of Eq. (1). The information amount IA_i will be calculated from Eq. (2). The information entropy (IE) is a product of both probability P_i and IA_i:

$$IE = P_i\, IA_i \tag{5}$$

The IE parameter is measured in bits and it varies between 0 and 1.

2.4. MAXIMUM INFORMATION ENTROPY

In the case of gas holdup fluctuations measured by means of a wire-mesh sensor [18], the fluctuations of the signal between the minimum and maximum values are divided into different zones with a progressively increasing height: 0.5, 2 × 0.5, 3 × 0.5, 4 × 0.5, etc. The maximum number of visits in a certain zone is determined. Fig. 1 below illustrates such a division. The maximum number of visits in a certain zone is presented on the right side of the figure in a grey box.

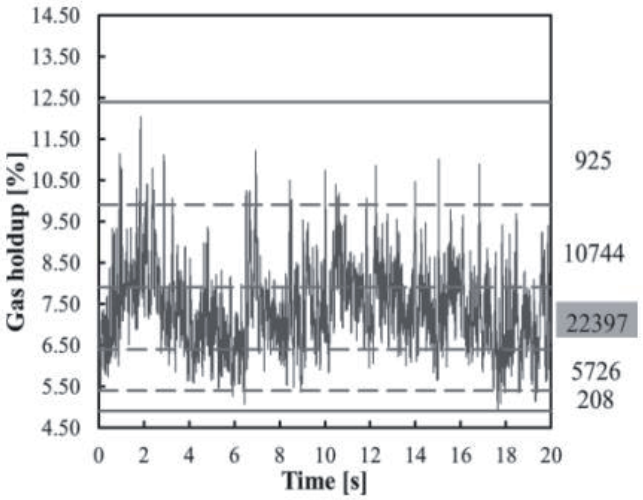

Fig. 1. Determination of maximum number of gas holdup visits in a single region in a large air-deionized water BC (0.4 m in ID).

Rys. 1. Określenie maksymalnej liczby wartości stopnia zatrzymania gazu obecnych w danym obszarze w kolumnie pracującej w układnie powietrze-woda dejonizowana (0,4 m średnicy).

Then Eqs. (2) is applied to calculate the probability as a ratio of this maximum number of visits divided by the practically possible maximum number visits (it was set at 30 000 visits based on analysis of different cases). The maximum information amount is calculated by means of Eq. (3) and the maximum information entropy (IE_{max}) is estimated by means of Eq. (5). Usually, the value of IE_{max} is much smaller than total IE.

3. EXPERIMENTAL SETUPS

3.1. MEASUREMENTS OF DIFFERENTIAL PRESSURE FLUCTUATIONS

The differential pressure (DP) fluctuations in a stainless steel column (0.102 m in ID; height: 2.4 m) operated with both nitrogen – tap water and nitrogen – ethanol (96 %) systems have been measured (at a sampling frequency of 100 Hz) at axial positions (z) of 0.65 and 1.15 m by means of a DP transducer (LABOM GmbH, Germany, range 0–1 bar). The other end of the DP transducer has been connected (by a common pipe) to the column top (see Fig. 2). This technique is nonintrusive since both ends of the DP transducer are mounted outside of the column. The clear liquid height has been kept constant at 1.7 m. A constant temperature has been maintained in the column (which was thermally insulated) by means of a thermostat. A perforated plate (PP) gas distributor consisting of 19 orifices with an ID of 1 mm has been used.

Before every measurement the gas flow rate has been pre-adjusted and then the waiting time (for flow stabilization) has been set at 120 s before the start of the real experiment. The KE algorithm (see section 2.1) has been successfully applied to the DP time series in order to extract useful hidden information about the U_g intervals of hydrodynamic stability.

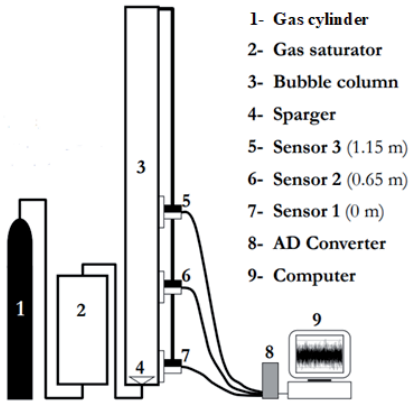

Fig. 2. Experimental BC facility for measuring the DP fluctuations in two gas-liquid systems.

Rys. 2. Schemat instalacji kolumny barbotażowej do pomiaru wahań ciśnienia różnicowego w dwóch układach gaz-ciecz.

3.2. MEASUREMENTS OF PHOTON COUNTS BY TOMOGRAPHIC SCANS

Nuclear gauge densitometry (NGD) facility has been used to record the photon counts in the middle of a BC (0.1 m in ID, 1.2 m in height) operated with an air-tap water systems at ambient conditions. Usually, such measurements are needed for estimating the radial gas holdup distribution at different axial positions. The gamma-ray source (Cs-137, 100 mCi) and the scintillation detector (cylindrical NaI crystal, 0.051 × 0.051 m) are mounted on a plate that could rotate around the column. In front of the scintillation detector has been placed a collimator ($(1.59 \times 10^{-3}$ m) × $(4.8 \times 10^{-3}$ m)). The photon count rate (based on a conversion from the output voltage) has been recorded by means of an automated data acquisition system. During every experiment, a focused beam of radiation has been transmitted from the source through the column walls and gas-liquid dispersion to the scintillation detector. The photon count fluctuations have been recorded at a sampling frequency of 50 Hz for a period of 300 s. NGD measures the spatial variation of the attenuation coefficient of gamma photons, which is linearly related to the gas holdup distribution. The schematic of the NGD facility and more details about it could be found in [19].

Computed tomography (CT) measurements have also been performed in a BC (0.162 m in ID, 2.5 m in height) operated with an air-therminol LT system at ambient conditions. The BC was equipped with a PP gas distributor (163 orifices × Ø 1.32 mm, open area=1.09 %). The CT scanner uses a Cesium (Cs-137) encapsulated gamma-ray source wih an activity of about 85 mCi. The array of five scintillation detectors and the sources are mounted on a gantry that can be rotated 360° around the column. Five scintialltion detectors (made of NaI) have been used. They have covered the entire cross-section of the column. Each detector consists of a cylindrical 0.051 × 0.051 m NaI crystal, a photo multiplicator and electronics, forming a 0.054 × 0.26 m cylindrical assembly. In each view, every detector acquires 7 projections covering a total angular span of 2.72° of the detector face. A total of 99 views were acquired, with 3.6° of angular shift after every view. Hence, 3465 projections (from 5 × 7 × 99) were used to reconstruct the phase holdup distribution at each cross-sectional plane. The entire system is completely automated to acquire the photon count data needed for the reconstruction of the phase holdup distribution in a given cross-section. 10 000 photon counts at every U_g value studied have been obtained. More details are available in [20].

3.3. MEASUREMENTS OF GAS HOLDUP FLUCTUATIONS

The measurements of the aerated liquid height (or the bubbling bed height) have been performed by means of a buoyancy device (made of a stainless steel for air- de-ionized water system) installed vertically downwards on a rod [21]. The lowest point of the buoyancy probe was fixed at 0.535 m. This value determines the lowest clear liquid height that can be used. A picture of the buoyancy device is shown in Fig.3a. When the U_g value increases and the bubble bed becomes more aerated, the buoyancy rises along

with the bubble bed surface and the time-dependent data about the aerated height are recorded. The sampling frequency has been set at 25 Hz. Such measurements have been performed in a BC (0.1 m in ID, see Fig. 3b) operated with an air–deionized water system. The BC facility together with the measurement buoyancy technique are available at the Engler-Bunte Institute, KIT (Germany).

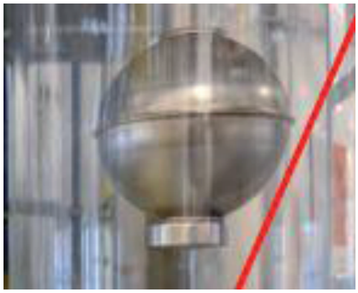

Fig. 3a. Photograph of the buoyancy device in an empty classical BC (0.1 m in ID).
The buoyancy device moves upwards on a rod with the liquid or gas-liquid dispersion.

Rys. 3a. Zdjęcie urządzenia wypornościowego w klasycznej kolumnie barbotażowej (0,1 m średnicy). Urządzenie wypornościowe porusza się w górę po pręcie wraz z dyspersją cieczową lub gazowo-cieczową.

A PP gas sparger (85 orifices × Ø 1.0 mm, open area = 0.85%) has been used. By means of an additional porous plate installed below the gas sparger, a uniform gas distribution has been ensured. If the porous plate is removed, a gas maldistribution can be observed at low U_g values. Below the PP gas sparger, a gas chamber (0.3 m in height) made of stainless steel has been installed. The clear liquid height H_0 has been fixed at 1.0 m. The gas holdup fluctuations have been treated by the NHI algorithm (see section 2.2) in order to identify precisely the hydrodynamically stable U_g ranges.

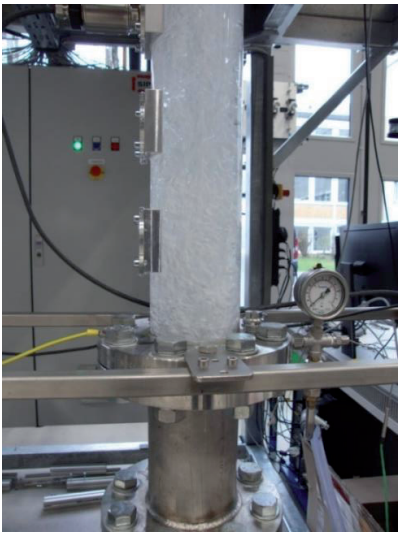

Fig. 3b. Photograph of the classical BC (0.1 m in ID) operated with an air-deionized water system.

Rys. 3b. Fotografia dolnej części klasycznej kolumny barbotażowej, pracującej w układzie powietrze-woda dejonizowana.

The gas holdup fluctuations have also been measured in a BC (0.15 m in ID) operated with an air-deionized water system at ambient conditions. The column was equipped with a PP gas distributor (14 orifices × Ø 4.0 mm, open area = 1.0 %). The clear liquid height has been adjusted at 2.0 m. The time series (60 000 points) of the cross-sectional averaged gas holdup (recorded as percentage) in the BC have been measured by means of a conductivity wire-mesh sensor (Fig. 4). The wire-mesh sensor consisted of two electrode planes each with 24 stainless-steel wires of 0.2×10^{-3} m and 6.125×10^{-3} m distance between the wires. The distance between the planes was 4.0×10^{-3} m and the wires from different planes crossed each other at right angles. This arrangement gave 576 crossing points, 78 % of them inside the cross-section of the column. One plane of the electrodes acted as a transmitter, the other one as a receiver. The transmitter electrodes were activated by a multiplexing circuit in successive order and signals derived from the current measured at the receiver electrodes were stored. After one multiplexing cycle, a two-dimensional matrix of values was available, reflecting the conductivities between all crossing points of the electrodes of the two perpendicular planes. The signals of the matrix were converted into gas holdup data based on proper calibration measurements on the liquid-flooded and empty column, respectively. The wire-mesh sensor was always installed at an axial position of 1.3 m above the gas distributor. More details can be found in [18].

Fig. 4. Photograph of the applied wire-mesh sensor with an ID of 0.15 m.

Rys. 4. Fotografia zastosowanego czujnika siatkowego o średnicy wewnętrznej 0,15 m.

3.4. TEMPERATURE FLUCTUATIONS IN AN ANNULARLY AERATED BC

The measurements have been performed in a facility consisting of an air compressor, air dryer, air filter, mass flowmeter (F-202AI MFC from Bronkhorst High-Tech) and an annularly aerated BC (for its dimensions see Fig. 5). Air–deionized water system at ambient pressure and temperature was used. The water was purified in the deionizing facility and the air was dried and compressed in the CompAir facility. The deionized water was introduced in the BC by means of a peristaltic pump.

The annularly aerated BC consisted of two concentric tubes (cylinders) made of PVC. The hydrodynamic behavior of the bubbly flow between the two concentric tubes has been investigated. The inner diameter (ID) of the external tube was 0.192 m and the height was 2.05 m, while for the internal tube the ID was 0.134 m, the outer diameter was 0.140 m and the height was 1.5 m, respectively. The clearance (see Fig. 5) between the BC bottom and the lower edge of the internal tube was 0.07 m. In principle, in the inner tube important heat removal equipment (in case of a high-temperature operation) could be installed. The gas distributor was installed only in the annulus and it contained 12 porous cylindrical needles (see Fig. 5) with dimensions 2.6×10^{-2} m in height and 1.3×10^{-2} m in diameter, made of small glass beads glued with a resin. The cylindrical needles have been separated by a regular distance in the annular section between the column inner wall and the internal tube's outer wall (see Fig. 5) and they were reaching height of 8.5×10^{-2} m over the column's bottom. The pores diameter was 90 μm. The bubbles generated by the 12 nozzles were rising only in the annulus.

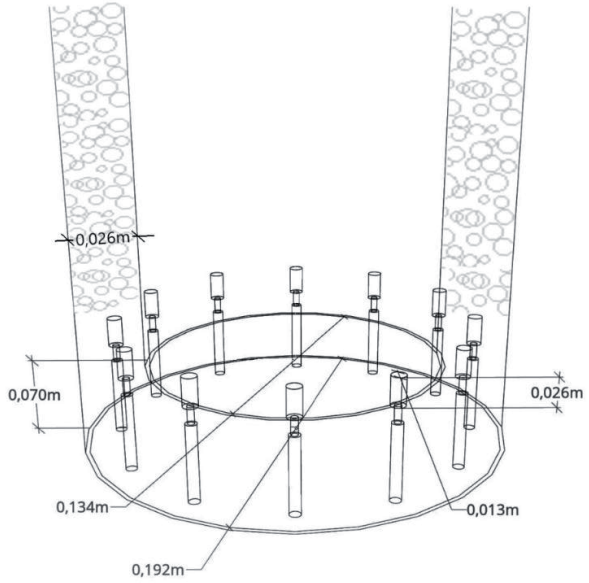

Fig. 5. Schematic of the lower part of the annularly aerated BC.

Rys. 5. Schemat dolnej części kolumny barbotażowej napowietrzanej pierścieniowo.

The initial (clear) liquid height was fixed at 1.05 m. In order to measure the temperature fluctuations a K-type thermocouple was used and was manufactured at the Institute's workshop. The thermocouple was located at an axial height (z) of 0.16 m above the bottom of the column. The temperature fluctuations were recorded with a time step of 1 second over a period of 10 minutes. Before every measurement the gas flow rate was pre-adjusted and then after 120 s (waiting time for flow stabilization) the signal recording started. The commercial thermocouples (for instance, from Omega Eng. (USA)) are also operating at a sampling frequency of 1 Hz. At the beginning and end of the measurement's day a water sample from the column was withdrawn and its temperature was measured by a standard thermometer. Then this temperature was compared with the reading of the K-type thermocouple. In most of the cases the temperature difference was only 0.1 °C. So, in this way it was confirmed that the thermocouple operates accurately. U_g values in the annulus in the range of 0.006 – 0.085 m/s were studied. The aerated bed heights were measured visually by means of a ruler glued to the column's wall in order to calculate the overall gas holdups.

4. RESULTS AND DISCUSSION

Most of the parameters characterizing the BC performance exhibit fluctuations at close (neighbouring) operating conditions. That is why, it is essential to introduce new parameters, which are stable in a certain U_g range and can be used for controlling and predicting the behavior of the gas-liquid dispersion in the column. In this section, such novel parameters extracted from different signals are summarized.

4.1. HYDRODYNAMICALLY STABLE AND SIMILAR CONDITIONS BASED ON DIFFERENTIAL PRESSURE FLUCTUATIONS

4.1.1. Nitrogen-ethanol system

In the case of the system nitrogen-ethanol (96 %) aerated in a BC (0.102 m in ID) equipped with a PP gas distributor (19 orifices × Ø 1 mm), the hydrodynamic stabilities (stable operation) and hydrodynamic similarities are listed in table 1a. A hydrodynamic stability is detected when there are at least three practically equal KE values at three close U_g values. The identification of such a U_g range is very important since within such a stable zone the BC behavior is fully predictable and controllable. Hydrodynamic similarities exist when only two operating conditions are characterized with the same KE values. Some hydrodynamic similarities are easy to understand. For instance, table 1a shows that the KE values are similar at U_g = 0.0206 and 0.0287 m/s (see case 1). The other similarity is at U_g = 0.0351 and 0.0396 m/s (see case 2). These operating conditions fall in the same (homogeneous) flow regime, which is characterized with the same flow pattern and similar mean bubble diameter.

The hydrodynamic stability at U_g values of 0.0407, 0.0454 and 0.0470 m/s (see case 3) is also easy to understand. The KE values are practically constant because all three U_g values belong to the same (transition) flow regime. Since these U_g values are beyond the main transition velocity U_{trans}, the practically constant KE values could be attributed to the constant holdup of the small bubbles (so-called dense phase holdup ε_{df}). According to the empirical correlation of Reilly et al. [22], the U_{trans} value is equal to 0.0259 m/s and the ε_{df} value is equal to 0.1352. The ε_{df} value in the heterogeneous regime depends only on the physicochemical properties of the gas-liquid system [22]:

$$\varepsilon_{df} = 4.457 \left(\frac{{\rho_G}^{0.96}}{\rho_L} {\sigma_L}^{0.12} \right)^{0.5} \tag{6}$$

It is noteworthy that similar dependence has been reported in [23].

Table 1a. Summary of both the hydrodynamic stabilities and similarities in the system nitrogen-ethanol (96 %) aerated in a BC (0.102 m in ID) at ambient conditions

Tabela 1a. Zestawienie hydrodynamicznych stabilności i podobieństw w układzie azot-etanol (96%) w kolumnie o średnicy 0,102m w warunkach otoczenia.

Case No.	U_g values, m/s	*KE* values, bits/s	Characterization of close conditions
1	0.0206	5.2050	Hydrodynamic similarity of 2 conditions
	0.0287	5.1833	
2	0.0351	5.0654	Hydrodynamic similarity of 2 conditions
	0.0396	5.0531	
3	0.0407	5.2653	
	0.0454	5.2556	Hydrodynamic stability of 3 conditions
	0.0470	5.2625	
4	0.0499	5.4145	
	0.0560	5.4208	Hydrodynamic stability of 4 conditions
	0.0686	5.4076	
	0.0733	5.3967	
5	0.0816	5.5202	Hydrodynamic similarity of 2 conditions
	0.1078	5.5301	
6	0.0861	5.6461	
	0.0917	5.6648	Hydrodynamic stability of 4 conditions
	0.0969	5.6476	
	0.0971	5.6427	

The Sauter-mean bubble diameter d_S is also very weakly dependent on the U_g value. Wilkinson et al. [24] argue that $d_S \sim U_g^{-0.02}$. The d_S value characterizes mainly the mean diameter of the small bubbles. For instance, in case 3 the d_S values are 3.545 mm, 3.537 mm and 3.535 mm, i.e. they are practically constant. In case 4 the d_S values are again practically constant: d_S=3.530 mm, 3.522 mm, 3.508 mm and 3.503 mm. In case 6 similar constant d_S trend is observed: d_S=3.492 mm, 3.488 mm, 3.484 mm and 3.484 mm, respectively.

Another set of four stable KE values is observed at U_g values between 0.0499 m/s and 0.0733 m/s (see case 4). This U_g range is around the onset of the heterogeneous flow regime. There are another two similar KE conditions at U_g values of 0.0816 and 0.1078 m/s (see case 5). They fall in the heterogeneous flow regime. Finally, the last stability set of four constant KE values is observed at high U_g values (between 0.0861 and 0.0971 m/s, see case 6). Under these highly turbulent conditions, even slugs might be observed.

Fig. 6a shows the three sets of hydrodynamically stable conditions listed in Table 1a. The second hydrodynamically stable U_g range is the widest one. In this zone, the BC operates in a fully predictable mode. Fig. 6a shows that the KE values in the three hydrodynamically stable U_g ranges gradually increase, which is due to increased liquid turbulence in the column.

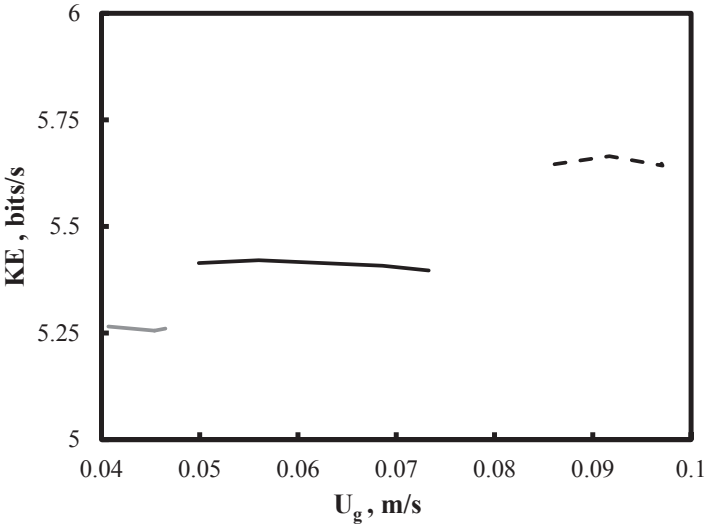

Fig. 6a. Graphical representastion of the three hydrodynamically stable U_g ranges listed in table 1a.

Rys. 6a. Graficzne przedstawienie trzech zakresów hydrodynamicznej stabilności wymienionych w tabeli 1a.

In summary, there are three hydrodynamic similarities between neighboring conditions in the KE profile and three sets of KE data that are characterized with a hydrodynamic stability. The stability conditions are the most interesting from the practical point of view. They occur beyond the main transition velocity U_{trans} (0.026 m/s), i.e. when the bubble coalescence begins and when the dense-phase gas holdup ε_{df} becomes constant [25]. The large bubbles are not stable and frequently they break up. It is reasonable to assume that in the identified stability conditions the break-up phenomenon prevails and mainly small bubbles (even in the column core) are observed. It is noteworthy that every new stability set of constant KE values is characterized with somewhat higher KE values, i.e. higher degree of chaotic and unpredictable behavior of the gas-liquid dispersion. So, the first hydrodynamic stability in case 4 is recommended for the best control of the BC performance. It falls in the transition flow regime.

4.1.2. Nitrogen-tap water system

In the case of nitrogen-tap water system, three U_g ranges characterized with hydrodynamic stability have been found. Table 1b shows that the first U_g range spans from 0.0206 m/s to 0.0308 m/s. It falls in the homogeneous flow regime since the first transition velocity U_{trans} occurs at 0.029 m/s [22]. The constant KE values in case 1 imply that the small bubble diameter is constant as predicted by Wilkinson et al. [24]. The second U_g range of hydrodynamic stability spans from 0.0659 m/s to 0.0780 m/s, i.e. in the heterogeneous flow regime. Again, the constant KE values in this U_g range can be explained with the constant dense phase holdup ε_{df} (0.1295) in this regime. The KE values start gradually to increase in comparison with case 1. It is noteworthy that the hydrodynamic stability in cases 1 and 2 comprises three U_g values. The third hydrodynamic stability range covers the U_g values from 0.0824 m/s to 0.0922 m/s. It is characterized with the highest KE values among the three hydrodynamic stability ranges. If hydrodynamic stability is needed in the homogeneous flow regime, then case 1 is recommended. On the contrary, when hydrodynamic stability in the heterogeneous flow regime is needed, then case 2 is recommended due to the lower KE values in comparison with case 3.

Table 1b. Summary of both the hydrodynamic stabilities and similarities in the system nitrogen-tap water aerated in a BC (0.102 m in ID) at ambient conditions

Tabela 1b. Zestawienie hydrodynamicznych stabilności i podobieństw w układzie azot-woda kranowa w kolumnie o średnicy 0,102 m w warunkach otoczenia.

Case No.	U_g values, m/s	*KE* values, bits/s	Characterization of close conditions
1	0.0206	5.1758	Hydrodynamic stability of 3 conditions
	0.0288	5.1839	
	0.0308	5.1988	
2	0.0659	5.7601	Hydrodynamic stability of 3 conditions
	0.0680	5.7919	
	0.0780	5.7711	
3	0.0824	6.2753	Hydrodynamic stability of 3 conditions
	0.0849	6.2368	
	0.0922	6.2750	

Fig. 6b shows the three sets of hydrodynamically stable conditions listed in table 1b. The first hydrodynamically stable U_g range is the smoothest one. In this zone, the BC operates in a fully predictable mode. Fig. 6b shows also that the KE values in the three hydrodynamically stable U_g ranges gradually increase, which is due to the increased liquid turbulence in the column. In comparison with Fig. 6a, it is observed that in a nitrogen-tap water system, there is no long U_g range of hydrodynamic stability and two of the intervals are not so smooth.

4.2. HYDRODYNAMICALLY STABLE CONDITIONS BASED ON PHOTON COUNTS ANALYSIS

It has been found that when the KE values are extracted from photon count fluctuations recorded by means of NGD [19] in an air-deionized water BC (0.1 m in ID), one set of hydrodynamically stable conditions and two sets of hydrodynamically similar conditions are observed. Table 2 shows that at U_g = 0.04, 0.06 and 0.08 m/s the KE values are more or less constant. This defines the first U_g range of hydrodynamic stability. All three U_g values fall in the heterogeneous flow regime since U_{trans}=0.029 m/s [22]. At U_g=0.025 m/s and 0.05 m/s similar KE values are observed and since the two

U_g values fall in the homogeneous and transition regimes this implies a similarity in the photon count fluctuations or maybe mean bubble sizes but not the flow patterns. Table 2 shows that the last hydrodynamic similarity occurs at U_g=0.045 m/s and 0.07 m/s. In this case, both U_g values fall in the heterogeneous flow regime.

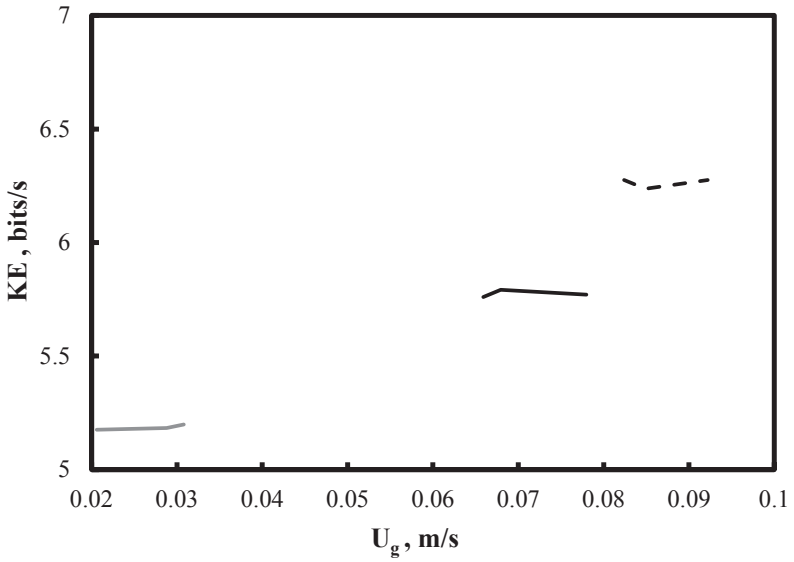

Fig. 6b. Graphical representastion of the three hydrodynamically stable U_g ranges listed in table 1b.

Rys. 6b. Graficzne przedstawienie trzech zakresów hydrodynamicznej stabilności wymienionych w tabeli 1b.

In the case of Computed Tomography (CT) [20] measurements in a BC (0.162 m in ID) operated with an air-therminol LT system at ambient conditions, Table 2 shows that two U_g ranges of hydrodynamic stability are observed. The first U_g range spans from 0.03 m/s to 0.08 m/s. It covers the transition and heterogeneous flow regimes since the U_{trans}=0.029 m/s for air-therminol LT system [22]. The first U_g range coincides with the one identified based on the NGD measurements in an air-deionized water BC (0.1 m in ID). The second hydrodynamically stable U_g range spans from 0.10 m/s to 0.14 m/s. Cases 2 and 3 from table 2 are graphically shown in Fig. 7.

Table 2. Summary of both the hydrodynamic stabilities and similarities based on photon count analysis in the system air-deionized water (NGD, BC diam.=0.10 m in ID) and air-therminol LT (CT, BC diam.=0.162 m in ID).

Tabela 2. Zestawienie hydrodynamicznych stabilności i podobieństw na podstawie analizy zliczeń fotonów w układach powietrze-woda dejonizowana i powietrze-terminol.

Case No.	U_g values, m/s	*KE* values, bits/s	Characterization of close conditions
1	0.04	4.2914	Hydrodynamic stability of 3 conditions
NGD	0.06	4.2534	
	0.08	4.2650	
2	0.03	0.3275	Hydrodynamic stability of 5 conditions
CT	0.04	0.3520	
	0.05	0.3328	
	0.06	0.3431	
	0.08	0.3711	
3	0.10	0.7381	Hydrodynamic stability of 4 conditions
CT	0.11	0.7414	
	0.13	0.7662	
	0.14	0.7540	

4.3. HYDRODYNAMICALLY STABLE CONDITIONS BASED ON GAS HOLDUP FLUCTUATIONS ANALYSIS

The gas holdup fluctuations have been recorded by means of a buoyancy device [21] in an air-deionized water BC (0.1 m in ID) operated at ambient conditions. Based on the extracted values of the new hybrid index (NHI), three U_g ranges with hydrodynamically stable conditions have been identified. Table 3 shows that the first U_g range comprises three operating conditions and falls in the heterogeneous flow regime (from $U_g = 0.0458$ m/s to $U_g = 0.0493$ m/s). The U_{trans} value for an air-deionized water system is equal to 0.029 m/s [22]. The second U_g range falls also in the heterogeneous flow regime (from $U_g = 0.0511$ m/s to $U_g = 0.0564$ m/s). The third U_g range with hydrodynamically stable operating conditions falls in the slug flow regime (from $U_g = 0.0846$ m/s to $U_g = 0.1057$ m/s). That is why, the NHI values are practically constant.

Table 3. Summary of both the hydrodynamic stabilities and similarities based on gas holdup fluctuations in the system air-deionized water (BC diam.=0.1 m) and air-benzonitrile (BC diam.=0.3 m)

Tabela 3. Zestawienie hydrodynamicznych stabilności i podobieństw na podstawie wahań stopnia zatrzymania gazu w układach powietrze-woda dejonizowana i powietrze-benzonitryl.

Case No.	U_g values, m/s	*NHI* values, –	Characterization of close conditions
1	0.0458	0.6946	
Water	0.0476	0.6990	Hydrodynamic stability of 3 conditions
	0.0493	0.7097	
2	0.0511	0.7501	
Water	0.0528	0.7488	Hydrodynamic stability of 4 conditions
	0.0546	0.7384	
	0.0564	0.7469	
3	0.0846	0.8826	
Water	0.0881	0.8900	
	0.0916	0.8863	Hydrodynamic stability of 6 conditions
	0.0951	0.8979	
	0.0987	0.9031	
	0.1057	0.9044	
4	0.0618	0.9045	
Benzo-nitrile	0.0637	0.9069	
	0.0680	0.8958	
	0.0741	0.9025	Hydrodynamic stability of 8 conditions
	0.0803	0.9057	
	0.0849	0.9074	
	0.0865	0.9098	
	0.0927	0.9136	

In the case of air-benzonitrile system aerated in a larger BC (0.3 m in ID), only one U_g range with hydrodynamically stable conditions has been identified. In the slug flow regime (U_g values from 0.0618 m/s to 0.0927 m/s) the NHI values are practically constant. There are no any other hydrodynamic stabilities or similarities. The U_{trans} value for an air-benzonitrile system is equal to 0.026 m/s [22].

Fig. 7 shows graphically the three hydrodynamically stable U_g ranges in an air-deionized water system, which are listed in table 3. In addition, the hydrodynamically stable conditions in the system air-benzonitrile are exhibited. It is clear that they are practically constant and this fact could be explained with the stability of the small bubble gas holdup in the heterogeneous regime. Fig. 7 shows that in the case of an air-deionized water system the NHI values above U_g=0.08 m/s are practically the same as the ones for the air-benzonitrile system. In this figure are also shown the CT values (air-therminol LT) from table 2, which are also practically constant.

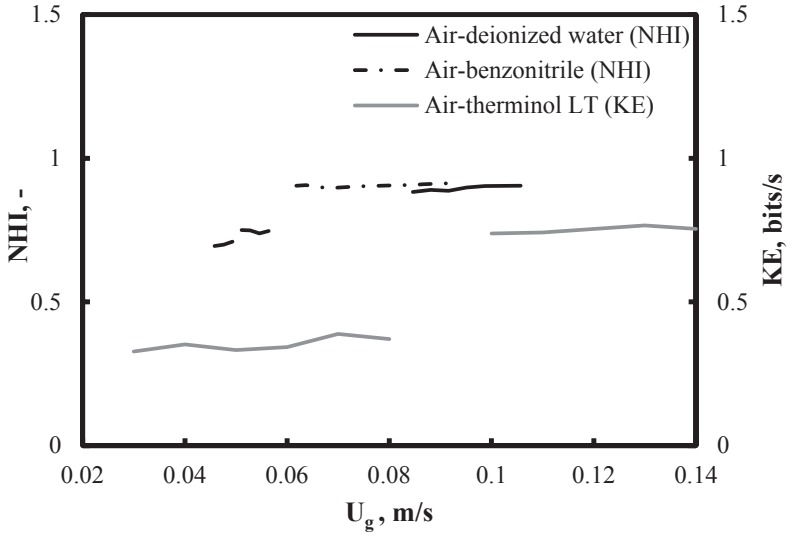

Fig. 7. Graphical representastion of the 3 hydrodynamically stable U_g ranges in air-deionized water and a stability set in air-benzonitrile system listed in table 3 and cases 2 and 3 (air-therminol LT) from table 2.

Rys. 7. Graficzne przedstawienie trzech zakresów hydrodynamicznej stabilności w układzie powietrze-woda dejonizowana oraz jeden zakres stabilności w układzie powietrze-benzonitryl wymienionych w tabeli 3 oraz przypadki 2 i 3 (układ powietrze-terminol) z tabeli 2.

In table 4 are summarized the five hydrodynamically stable conditions obtained from IE_{max} values extracted from gas holdup fluctuations recorded by a wire-mesh sensor in an air-deionized water system. Five practically constant IE_{max} values are observed in the heterogeneous regime and this implies that slugs are being formed at these high

U_g values due to the relatively narrow column diameter (0.15 m). The U_{trans} value for an air-deionized water system is equal to 0.029 m/s [22].

Table 4. Summary of the hydrodynamically stable conditions based on gas holdup data (in an air-deionized water system) from a wire-mesh sensor.
Tabela 4. Zestawienie warunków hydrodynamicznej stabilności opartych na wartościach stopnia zatrzymania gazu (w układzie wody dejonizowanej powietrzem) z czujnika siatkowego.

Case No.	U_g values, m/s	IE_{max} values, bits	Characterization of close conditions
1	0.0788	0.1334	Hydrodynamical stability of 5 conditions
	0.1009	0.1420	
	0.1124	0.1392	
	0.1239	0.1392	
	0.1344	0.1351	

4.4. HYDRODYNAMICALLY STABLE AND SIMILAR CONDITIONS BASED ON TEMPERATURE FLUCTUATIONS IN AN ANNULARLY AERATED BC

When the total IE values are extracted from temperature fluctuations recorded in an annularly aerated BC (annular gap: 0.026 m) operated with an air-deionized water system at ambient conditions, then only one hydrodynamically stable U_g range is observed. Table 5 shows that it spans from 0.0128 m/s to 0.0319 m/s, i.e. in the homogeneous flow regime. The U_{trans} value for an air-deionized water system is equal to 0.029 m/s [22]. Six practically constant IE values are observed. In addition, three sets of hydrodynamically similar conditions are detected. The first hydrodynamic similarity is between $U_g = 0.0064$ m/s and 0.0349 m/s. These conditions fall in the homogeneous flow regime and the IE values are practically constant at about 0.59 bits. The second hydrodynamical similarity is observed in the heterogeneous regime: at $U_g = 0.0555$ m/s and 0.0758 m/s. The IE values are practically constant at about 0.680 bits. The third hydrodynamical similarity occurs at $U_g = 0.0583$ m/s and 0.0735 m/s. The IE values are practically constant at about 0.635 bits.

Table 5. Summary of both the hydrodynamic stabilities and similarities based on temperature fluctuations in an annularly aerated BC operated with an air-deionized water system

Tabela 5. Zestawienie hydrodynamicznych stabilności i podobieństw opartych na wahaniach temperatury w kolumnie barbotażowej napowietrzanej pierścieniowo, pracującej w układzie powietrze-woda dejonizowana.

Case No.	U_g values, m/s	*IE* values, bits	Characterization of close conditions
1	0.0128	0.7543	Hydrodynamic stability of 6 conditions
	0.0160	0.7643	
	0.0223	0.7526	
	0.0255	0.7565	
	0.0287	0.7465	
	0.0319	0.7685	
2	0.0064	0.5924	Hydrodynamic similarity of 2 conditions
	0.0349	0.5929	
3	0.0555	0.6800	Hydrodynamic similarity of 2 conditions
	0.0758	0.6857	
4	0.0583	0.6341	Hydrodynamic similarity of 2 conditions
	0.0735	0.6388	

CONCLUSIONS

The identification of hydrodynamically stable conditions in bubble columns (BCs) is very important for their successful operation and the reliable control of their behavior. In this work, the following hydrodynamically stable conditions based on various recorded signals (differential pressure fluctuations, photon counts, gas holdup fluctuations and temperature fluctuations) and different parameters (KE, NHI and IE) have been detected.

- In the case of DP fluctuations in a nitrogen-ethanol (96 %) and nitrogen-tap water systems aerated in a BC (0.102 m in ID), based on the KE values three different sets of hydrodynamically stable conditions have been identified.
- In the case of KE values extracted from photon counts recorded in an air-deionized water BC (0.1 m in ID) and photon counts recorded in an air-therminol BC (0.162 m in ID), the same hydrodynamically stable U_g range (0.03 m/s – 0.08 m/s) has been detected. One additional set of hydrodynamically stable conditions has been found for the air-therminol LT system.
- The new hybrid indices (NHI) extracted from gas holdup fluctuations in an air-deionized water BC (0.1 m in ID) and in an air-benzonitrile BC (0.3 m in ID) are capable of identifying one U_g range of hydrodynamic stability. In the first case it falls in the heterogeneous regime, while in the second it falls in the slug flow regime. The maximum information entropies extracted from data measured by a wire-mesh sensor are capable of identifying one hydrodynamically stable zone.
- In an annularly aerated BC (annular gap: 0.026 m) operated with an air-deionized water system, the information entropies (IE) are capable of identifying only one U_g range of hydrodynamic stability.

The identified hydrodynamically stable conditions are very useful for selecting an optimal operational U_g range of the BC, which is characterized with better control and predictability. For instance, in the case of KE values, it should be selected the U_g range with the lower KE values. This practical rule should be applied by considering the need to operate the column either in the homogeneous or heterogeneous flow regimes.

SYMBOLS – OZNACZENIA

AAD	– average absolute deviation, mbars or – średnie odchylenie bezwzględne
b	– number of steps before two vectors deviate from each other, – liczba kroków, zanim dwa wektory odchylią się od siebie
b_{avg}	– average number of vector pairs with a distance smaller than AAD, – średnia liczba par wektorów o odległości mniejszej niż AAD
IA	– information amount, bits ilość informacji
IE	– information entropy, bits entropia informacji
IE_{max}	– maximum information entropy, bits maxymalna entropia informacji
KE	– Kolmogorov entropy, bits/s entropia Kołmogorowa
N	– total number of points in time series, – łączna liczba punktów w szeregach czasowych
NHI	– new hybrid index, – nowy indeks hybrydowy
P	– probability for repetition of certain value or maximum visits in a region, –

prawdopodobieństwo powtórzenia określonej wartości lub maksymalnej liczby pobytów w regionie

U_g – superficial gas velocity, m/s
powierzchniowa prędkość gazu

U_{trans} – transitional gas velocity, m/s
przejściowa prędkość gazu

x – point in the time series, –
punkt w szeregu czasowym

x_{mean} – mean of all points in the time series, –
średnia wszystkich punktów w szeregach czasowych

z – axial position, m
położenie osiowe

ε_{df} – dense-phase gas holdup, –
stopień zatrzymania gazu "małych pęcherzyków

ρ_G – gas density, kg/m^3
gęstość gazu

ρ_L – liquid density, kg/m^3
gęstość cieczy

σ_L – liquid surface tension, N/m
napięcie powierzchniowe cieczy

ABBREVIATIONS –SKRÓTY

BC – bubble column
kolumna barbotażowa

BSD – bubble size distribution
rozkład średnic pęcherzyków

CT – computed tomography
tomografia komputerowa

ID – inner diameter
średnica wewnętrzna

NGD – nuclear gauge densitometry
densytometria jądrowa

PP – perforated plate
płyta perforowana

REFERENCES – PIŚMIENNICTWO CYTOWANE

[1] Barati-Harooni, A., Jamialahmadi, M., 2021. Experimental investigation and correlation of the effect of carbon nanotubes on bubble column fluid dynamics: gas holdup, flow regime transition, bubble size and bubble rise velocity. Int. J. Multiph. Flow, 139, 103647. DOI: 10.1016/j.ijmultiphaseflow.2021.103647.

[2] Kantarci, N., Borak, F., Ulgen, K. O., 2005. Bubble column reactors. Process Biochem., 40 (7), 2263–2283. DOI: 10.1016/j.procbio.2004.10.004.

[3] Manjrekar O. N., Duduković, M. P., 2019. Identification of flow regime in a bubble column reactor with a combination of optical probe data and machine learning technique. Chem. Eng. Sci., X(2), 100023, DOI: 10.1016/j.cesx.2019.100023.

[4] Vial, C., Poncin, S., Wild, G., Midoux, N., 2001. A simple method for regime identification and flow characterisation in bubble columns and airlift reactors. Chem. Eng. Process., 40(2), 135–151, 2001, DOI: 10.1016/S0255-2701(00)00133-1.

[5] Nedeltchev, S., Hampel, U., Schubert, M., 2016. Investigation of the radial effect on the transition velocities in a bubble column based on the modified shannon entropy. Chem. Eng. Res. Des., 115, 303–309. DOI: 10.1016/j.cherd.2016.08.011.

[6] Lucas D., Ziegenhein, T., 2019. Influence of the bubble size distribution on the bubble column flow regime. Int. J. Multiph. Flow, 120, 103092, DOI: 10.1016/j.ijmultiphaseflow.2019.103092.

[7] Olmos, E., Gentric, C., Poncin, S., Midoux, N., 2003. Description of flow regime transitions in bubble columns via laser Doppler anemometry signals processing. Chem. Eng. Sci., 58 (9), 1731–1742, DOI: 10.1016/S0009-2509(03)00002-2.

[8] Leonard, C.. Ferrasse, J.-H., Boutin, O., Lefevre, S., Viand, A., 2015. Bubble column reactors for high pressures and high temperatures operation. Chem. Eng. Res. Des., 100, 391–421, DOI: http://dx.doi.org/10.1016/j.cherd.2015.05.013.

[9] De Swart, J. W. A., Van Vliet, R. E., Krishna, R., 1996. Size, structure and dynamics of 'large' bubbles in a two-dimensional slurry bubble column. Chem. Eng. Sci., 51 (20), 4619–4629, DOI: 10.1016/0009-2509(96)00265-5.

[10] Bhole, M. R., Joshi, J. B., 2005. Stability analysis of bubble columns: predictions for regime transition. Chem. Eng. Sci., 60 (16), 4493–4507, DOI: 10.1016/j.ces.2005.01.004.

[11] Krishna, R., 2000. A scale-up strategy for a commercial scale bubble column slurry reactor for fischer-tropsch synthesis. Oil Gas Sci. Technol., 55 (4), 359–393, DOI: 10.2516/ogst:2000026.

[12] Nedeltchev, S., Top, Y., Hlawitschka, M., Schubert, M., Bart, H.-J., 2020. Identification of the regime boundaries in bubble columns based on the degree of randomness in the signals. Can. J. Chem. Eng., 98(7), 1607–1621, DOI: 10.1002/cjce.23719.

[13] Besagni, G., Inzoli, F., 2017. The effect of liquid phase properties on bubble column fluid dynamics: gas holdup, flow regime transition, bubble size distributions and shapes, interfacial areas and foaming phenomena. Chem. Eng. Sci., 170, 270–296, DOI: 10.1016/j.ces.2017.03.043.

[14] Gan, Z. W., Yu, S. C. M., Law, A. W. K., 2011. Hydrodynamic stability of a bubble column with a bottom-mounted point air source. Chem. Eng. Sci., 66, 5338–5356, DOI: 10.1016/j.ces.2011.07.032.

[15] Van den Bleek, C. M., Schouten, J. C., 1993. Deterministic chaos: a new tool in fluidized bed design and operation. Chem. Eng. J., 53, 75-87.

[16] Schouten, J. C., Takens, F., Van den Bleek, C. M., 1994. Maximum-likelihood estimation of the entropy of an attractor, Phys. Rev. E Stat. Phys Plasmas Fluids Relat. Interdisc. Top., 49, 126-129.

[17] Letzel, H. M., Schouten, J. C., Krishna, R., Van den Bleek, C. M., 1997. Characterization of regimes and regime transitions in bubble columns by chaos analysis of pressure fluctuations. Chem. Eng. Sci., 52, 4447-4459.

[18] Nedeltchev, S., Rabha, S., Hampel, U., Schubert, M., 2015. A new statistical parameter for identifying the main transition velocities in bubble columns. Chem. Eng. Techn., 38(11), 1940-1946, DOI: 10.1002/ceat.201400728.

[19] Nedeltchev, S., Shaikh, A., Al-Dahhan, M., 2011. Flow regime identification in a bubble column via nuclear gauge densitometry and chaos analysis. Chem. Eng. Techn., 34(2), 225-233, DOI: 10.1002/ceat.201000308.

[20] Nedeltchev, S., Shaikh, A., Al-Dahhan, M., 2006. Flow regime identification in a bubble column based on both statistical and chaotic parameters applied to computed tomography data. Chem. Eng.Techn., 29(9), 1054-1060, DOI: 10.1002/ceat.200600162.

[21] Mörs, F., Ortloff, F. Graf, F., Kolb, T., 2019. Hydrodynamik in blasensäulen-messung von relativem gasgehalt und blasengröße. Chemie Ingenieur Tech., 91, 1059–1065.

[22] Reilly, I. G., Scott, D. S., De Bruijn, T. J. W., MacIntyre, D., 1994. The role of gas phase momentum in determining gas holdup and hydrodynamic flow regimes in bubble column operations. Can. J. Chem. Eng., 72, 3-12.

[23] Wilkinson, P. M., Spek, A. P., Van Dierendonck, L. L., 1992. Design parameters estimation for scale up of high pressure bubble columns. AIChE J., 38, 544-554.

[24] Wilkinson, P. M., Haringa, H., Van Dierendonck, L. L., 1994. Mass transfer and bubble size in a bubble column under pressure. Chem. Eng. Sci., 49, 1417-1427.

[25] Krishna, R., Ellenberger, J., 1996. Gas holdup in bubble column reactors operating in the churn-turbulent flow regime. AIChE J. 42, 2627-2634.

STOYAN NEDELTCHEV, JAKUB KATERLA

WYZNACZENIE ŁATWO PRZEWIDYWALNYCH I HYDRODYNAMICZNIE STABILNYCH WARUNKÓW W RÓŻNYCH KOLUMNACH BARBOTAŻOWYCH

Niezawodna i stabilna hydrodynamicznie praca kolumn barbotażowych (BC) jest niezwykle istotna dla ich skutecznego projektowania, kontroli i zwiększania skali. W heterogenicznym reżimie przepływu (FR) występują dwa konkurencyjne procesy: koalescencja (łączenie) i rozpad pęcherzyków. Zjawiskiem pożądanym jest równowaga między tymi procesami, jednak w wielu przypadkach jeden z wymienionych procesów przeważa. Złączone pęcherzyki o dużych rozmiarach są niestabilne i często rozpadają się na mniejsze pęcherzyki o większej stabilności. W niniejszej pracy warunki hydrodynamicznej stabilności, definiowane jako te stosunkowo bliskie powierzchniowej prędkości gazu U_g, charakteryzowano przez kilka (3-8) praktycznie stałych wartości oznaczanych parametrów (entropia Kołmogorowa (KE), nowy indeks hybrydowy (NHI), czy entropia informacji (IE)). W większości z zidentyfikowanych przypadków, zakresy hydrodynamicznej stabilności zawierają trzy lub cztery wartości U_g. Praktycznie stałe wartości badanych parametrów zostały przypisane do stałego stopnia zatrzymania „małych pęcherzyków" w heterorežimie. Warunki hydrodynamicznego podobieństwa zostały zidentyfikowane we wszystkich trzech reżimach. Warunki te odpowiadają dwóm różnym wartościom U_g, które są charakteryzowane przez te same wartości badanych parametrów. Gdy wartości U_g należą do różnych reżimów, to podobieństwa są powiązane z podobnymi fluktuacjami sygnałów.

Analizowano cztery różne przypadki. W pierwszym wartości KE pozyskano z pomiarów ciśnienia różnicowego rejestrowanych w kolumnie o średnicy 0,102 m, pracującej w układnie azot-etanol (96 %) lub azot-woda kranowa. W przypadku etanolu zidentyfikowano trzy zakresy U_g hydrodynamicznie stabilne oraz trzy zakresy hydrodynamicznego podobieństwa. W przypadku wody kranowej, wyznaczono również trzy przedziały hydrodynamicznej stabilności.

W kolejnym przypadku wartości KE ekstrahowano ze zliczeń fotonów mierzonych za pomocą densytometrii jądrowej w kolumnie (0,10 m średnicy; azot-woda kranowa). Zidentyfikowano trzy zakresy hydrodynamicznej stabilności występujące w reżimie heterogenicznym. Ponadto oznaczono jeden zakres hydrodynamicznej stabilności na podstawie danych, pochodzących z czujnika siatkowego drucianego. W układzie powietrze-terminol LT w kolumnie o średnicy równej 0,162 m znaleziono te same zakresy U_g dla warunków hydrodynamicznej stabilności. Ponadto w wyższych wartościach powierzchniowej prędkości gazu wyznaczono jeden dodatkowy przedział hydrodynamicznej stabilności (w reżimie przepływu tłokowego – wysokie wartości U_g).

W trzecim przypadku wartości NHI pozyskano ze zmian stopnia zatrzymania gazu mierzonego za pomocą urządzenia wypornościowego. Badanie prowadzono w układzie powietrze-woda dejonizowana w kolumnie o średnicy 0,1 m. W reżimie heterogenicznym zidentyfikowano trzy zestawy warunków hydrodynamicznej stabilności. W większej kolumnie o średnicy wewnętrznej 0,3 m, pracującej w układzie powietrze-benzonitryl, oznaczono jeden zakres U_g hydrodynamicznie stabilny.

Ostatecznie, czwarty z parametrów – IE – ekstrahowano z pomiarów temperatur rejestrowanych w napowietrzanej pierścieniowo kolumnie. Zidentyfikowano jeden hydrodynamicznie stabilny zakres U_g w homogenicznym reżimie przepływu i trzy zakresy hydrodynamicznego podobieństwa w różnych reżimach przepływu.

Received: 08.11.2021
Accepted:23.12.2021